Supplementary Materials

Efficient selective hydrogenation of phenylacetylene over Pd-based rare earth dual-atomic catalysts

Leisheng Che[1,#], Ziyun Zhong[1,#], Peng Cui[2], Yaping Du[1,*], Hongbo Zhang[1,*]

[1]School of Materials Science and Engineering, Tianjin Key Laboratory for Rare Earth Materials and Applications, Haihe Laboratory of Sustainable Chemical Transformation, Nankai University, Tianjin 300350, China

[2]Key Laboratory of Functionalized Molecular Solids, Ministry of Education, Anhui Laboratory of Molecule-based Materials, College of Chemistry and Materials Science, Anhui Normal University, Wuhu 241002, Anhui, China.

[#]Authors contributed equally.

[*]**Correspondence to:** Prof. Hongbo Zhang, Prof. Yaping Du, School of Materials Science and Engineering, Tianjin Key Laboratory for Rare Earth Materials and Applications, Haihe Laboratory of Sustainable Chemical Transformation, Nankai University, No.38 Tongyan Road, Jinnan District, Tianjin 300350, China.
hbzhang@nankai.edu.cn; ypdu@nankai.edu.cn

Contents

1. Experimental procedure

1.1. XRD of 0.02%Pd-Ln/C (Ln = Y/Lu) catalysts

X-ray diffraction (XRD) patterns of 0.02%Pd-Ln/C (Ln = Y/Lu) catalysts were recorded on a Rigaku Smart Lab 3 kW diffractometer operating at 40 kV and 40 mA equipped with a CuKα radiation source (λ= 0.15418 nm). The scanning rate was $5°\cdot min^{-1}$.

1.2. TEM of Pd-Y/C catalysts

Transmission electron microscopy (TEM) with EDS spectroscopy of Pd-Y/C catalysts with different Pd loading were determined on JEOL JEM-2800 microscope, which was operated at an accelerating voltage of 200 kV with 0.21 nm resolution. The samples were suspended in ethanol by ultra-sonication. Then the suspension was dropped onto the copper grid for TEM measurements.

1.3. HAADF-STEM of 0.02%Pd-Y/C and 0.5%Pd-Y/C catalysts

High-angle annular dark-filed scanning TEM (HAADF-STEM) of 0.02%Pd-Y/C and 0.5%Pd-Y/C catalysts were conducted on a JEOL JEM-ARM200F microscope, which was operated at an accelerating voltage of 200 kV with 0.11 nm information resolution functionalized with a probe Cs corrector.

1.4. XAFS analysis of 0.5%Pd-Y/C and 0.5%Pd/C catalysts

On the BL14W Beam line of Shanghai Synchrotron Radiation Facility (SSRF) (Shanghai, China), the XAFS analysis of Pd K-edge and Y K-edge was performed with Si(111) crystal monochromators. Before the analysis at the beamline, samples were placed within the aluminum sample holders and sealed with a Kapton tape film. The XAFS spectra were recorded at room temperature using a 4-channel Silicon Drift Detector (SDD) Bruker 5040. Pd K-edge and Y K-edge extended X-ray absorption fine structure (EXAFS) spectra were recorded in transmission/fluorescence mode. Negligible changes in the line-shape and peak position of Pd K-edge and Y K-edge XANES spectra were determined between two scans taken for a specific sample. The XAFS spectra of these standard samples were recorded in transmission mode. The spectra were processed and analyzed by the software codes Athena [1].

1.5. Gas adsorption measurements

The adsorption isotherms of H_2 were obtained on a TriStar II 3020 Version 3.02 gas adsorption instrument. The 0.02%Pd-Y/C catalyst was degassed at 473 K under dynamic vacuum for 10 h prior to the gas adsorption measurements. A circulator bath was applied to maintain the required temperature.

The differential enthalpies (ΔH) and entropies of adsorption (ΔS) were estimated as a function of H_2 gas adsorption from isotherms that were determined at 273 K and 298 K using the van't Hoff isochore:

$$\ln P = \frac{\Delta H}{RT} - \frac{\Delta S}{R} \qquad (S\,1)$$

Where P is pressure, T is the temperature, R is the real gas constant. Liner fitting of the plot of lnP versus 1/T at constant gas loading allows the differential enthalpy (ΔH) and entropies of adsorption (ΔS) to be determined from the slope and the intercept of the line, respectively.

2. Characterization of catalysts

2.1. Schematic illustration of synthesis of Pd-Y/C catalyst

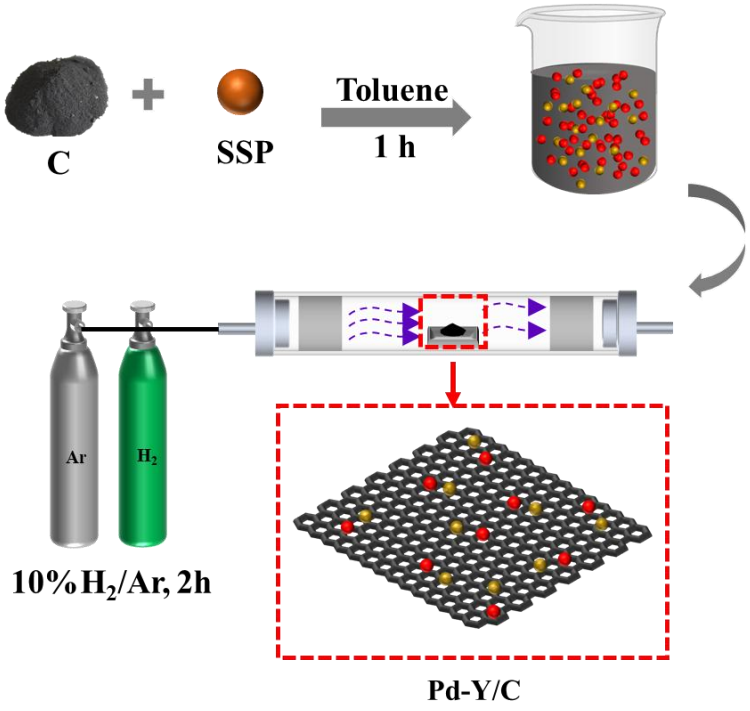

Supplementary Figure 1. Schematic illustration of synthesis of Pd-Y/C catalyst.

2.2. XRD results

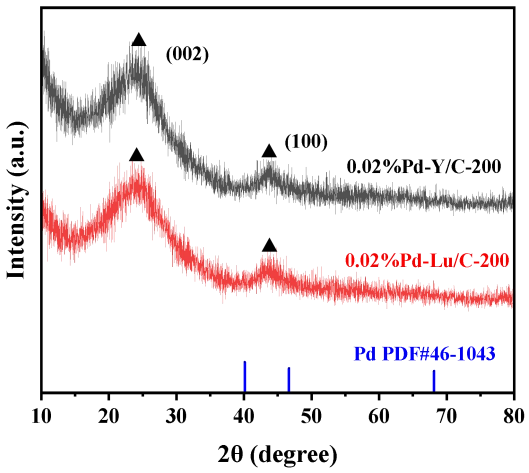

Supplementary Figure 2. XRD patterns at 10-80° of 0.02%Pd-Ln/C (Ln = Y/Lu) catalysts.

2.3. Catalytic performance

Supplementary Table 1. Summary of the latest development of catalytic hydrogenation of phenylacetylene over different catalysts

Catalyst	Pd loading	Amount of catalyst	C_8H_6 conversion (%)	C_8H_8 selectivity (%)	Reference
Pd_1/Ni@G	0.098%	25mg	100	93	[2]
Pd_1/TiO_2	0.203%	25mg	99	91	[3]
Pd-Ru@ZIF-8	0.7%	2.5mg	98	96	[4]
Pd@mpg-C_3N_4	0.67%	50mg	93	89	[5]
$Pd_{4.5}Se$ NCs	3%	5mg	100	98	[6]
Pd-Zn@MS	-	2.5mg	95	92	[7]
Pt-Cu/C	1%(Pt)	100mg	100	94.4	[8]
Pt-Cd-700	4.2%(Pt)	0.6mg Pt	100	86.2	[9]
Au/GO	2%(Au)	30mg	99	99	[10]

Supplementary Table 2. Phenylacetylene hydrogenation performance over different Pd-based catalysts

Catalyst	Pd loading	Amount of catalyst	T (°C)	P (bar)	Space velocity[a]	Conv. (%)	Sele. (%)	TOR (mmol /g_{cat}/h)	TOF[b] (h^{-1})	Ref.
Pd@carbon	1%	10mg	50	2	750 rpm	85	88	-	-	[15][11]
2.5Au-Pd@mpg-C_3N_4	5.64%	10mg	30	1	-	29	96	-	-	[5]
Pd@γ-Al_2O_3	5.64%	10mg	30	1	-	99	90	-	-	[5]
Pd@TiO_2	1%	10mg	30	5	-	100	86	396000	73080	[16][12]
Pd@MgO	5.64%	10mg	30	1	-	99	91	-	-	[5]
Pd@CeO_2	5.64%	10mg	30	1	-	95	91	-	-	[5]
Pd+PEI(L)@HSS	4.6%	50mg	30	1	600 rpm	99	84	-	4111	[17][13]
Pd/FDU-12	0.78%	3μmol Pd	25	1	-	60	95	-	-	[18][14]
Pd/PPh3@FDU-12	0.83%	0.003mmol Pd	25	1	-	92	94	-	-	[18][14]
Pd/CuS	0.37%	5.4 μmol Pd	70	5	800 rpm	90.3	91.1	-	-	[19][15]
Pd/C (10wt%)	10%	5mg	RT	3	-	100	32	8.16	865	[3]
1.5Pd-TiO_2 (150 °C)	1.505 %	3.3mg	RT	10	-	98	85	8.08	5730	[3]
0.5Pd-TiO_2 (150 °C)	0.497 %	10mg	RT	10	-	97	88	2.97	6317	[3]

0.2Pd/TiO_2 (150 °C)	0.203 %	25mg	RT	10	-	99	91	1.62	8596	[3]
0.2Pd-TiO_2 (post-150 °C)	0.203 %	25mg	RT	10	-	79	86	1.29	6772	[3]
Pd Lindlar catalyst	5%	10mg	60	10	-	99	87	2.02	214	[3]
Pd(0)-AmP-HSNs	13.1%	2.44mg	RT	1	-	93	89	-	106	[20][16]
Pd/Al-MCM-41	1%	5mg	50	1	1400 rpm	100	96	-	3636	[21][17]
CN-Pd-1.4	1.4%	5mg	25	1	-	99.9	91.3	-	4544	[22][18]
CN-Pd-3.0	3%	5mg	25	1	-	99.9	78.2	-	1060	[22][18]
PdZn+0.25Pb	1%	10mg	RT	1	-	99	94	102	450	[23][19]
Ni/Pd (50:50)	0.53%	2mg	50	30	-	100	96.6	-	5256	[24][20]
Fe/Pd (50:50)	0.51%	2mg	50	30	-	100	96.5	-	4392	[24][20]
Mg/Pd (50:50)	0.75%	2mg	50	30	-	100	94	-	3888	[24][20]
$Pd_{0.33}Pb_{0.67}$/C	1.98%	5mg	30	1	-	99	97	-	482	[25][21]
Pd_1/Ni@G	0.098 %	25mg	30	2	-	100	93	-	7074	[12][22]
Pd-Ru@ZIF-8	0.7%	2.5mg	100	1	-	98	96	-	2188	[4]
Pd@mpg-C_3N_4	0.67%	50mg	30	1	-	93	89	-	-	[5]
$Pd_{4.5}Se$ NCs	3%	5mg	110	1	800 rpm	100	98	-	351.4	[6]

Pd-Zn@MS	-	2.5mg	100	1	-	95	92	-	-	[7]
Pd/NTs	0.66%	150mg	50	1	800 rpm	100	97	-	3456	[26][23]
0.02%Pd-Y/C	0.02%	20mg	120	1	25.4 h^{-1}	100	92	2.2	-	This work

[a] Except for the gas phase reaction in this work, all references are liquid phase reactions. In this work, the space velocity is the weight hourly space velocity (WHSV), while in the literature, the space velocity is the revolutions per minute (rpm).

[b] Most Pd based catalysts in the literature did not report turnover rate (TOR), but instead reported turnover frequency (TOF).

"-" represents no reports in the literature.

Supplementary Table 3. Stability of phenylacetylene hydrogenation over various Pd-based catalysts

Catalyst	Pd loading	Amount of catalyst	Reaction conditions	Recycle number	TOS (h)	Ref.
Pd@mpg-C_3N_4	0.67%	50mg	29.25 mmol C_8H_6; 50 mg catalyst; 150 mL ethanol; 303 K; 1 bar H_2	9	16.8	[5]
Pd+PEI (L)@HSS	4.6%	50mg	1 mmol C_8H_6; catalyst (Pd 0.5 mol %); 10 mL (MeOH:1,4-dioxane = 1:1); 303 K; 1bar H_2;	5; 3 h/cycle	15	[17][13]
Pd/PPh3@FDU-12	0.83%	3 μmol Pd	1.8 mmol C_8H_6; S/C =1000; 5 mL EtOH; 298K; 1 bar H_2;	5; 1.33 h/cycle	6.67	[18][14]
Pd/CuS	0.37%	5.4 μmol Pd	0.2 mmol C_8H_6; 9 mL ethyl acetate; 0.5 MPa H2; 343 K; 7h	6	7	[19][15]
CN-P-Pd-1.4	1.4%	5mg	1.5 mmol C_8H_6; 5 mg catalyst; 15 mL methanol; 298 K; 0.5 h; 1 bar H_2	5; 0.5 h/cycle	2.5	[22][18]
$Pd_{0.33}Pb_{0.67}$/C	1.98%	5mg	0.91 mmol C_8H_6; 5 mg catalyst; 5 mL acetonitrile; 303K; 1bar H_2	5; 2 h/cycle	10	[25][21]
Pd_1/Ni@G	0.098%	25mg	1.85 mmol C_8H_6; 25 mg catalyst; 303 K; 2 bar H_2; 10 mL ethanol	5; 1.08 h/cycle	5.4	[2]
Pd-Ru@ZIF-8	0.7%	2.5mg	0.3 mmol C_8H_6; 2.5 mg catalyst; 25 mL ethanol; 373 K,	5; 2 h/cycle	10	[4]

			2h, 1bar H_2			
	3%	5mg	0.5 mmol C_8H_6;			
$Pd_{4.5}Se$ NCs			5mL DMF;	10; 1.5	15	[6]
			nPd/nC_8H_6=0.28%;	h/cycle		
			383K; 0.1 MPa H_2;			
	-	2.5mg	0.3 mmol C_8H_6;			
Pd-Zn@MS			2.5 mg catalyst; 25	5; 1.67	8.3	[7]
			mL EtOH; 373K; 1	h/cycle		
			bar H_2			
	0.02%	20mg	30 kPa H_2, 0.3 kPa			
0.02%Pd-Y/C			C_8H_6, 2.784 kPa	40; 0.5	20	This
			C_6H_{12}, balance	h/cycle		work
			with Ar, WHSV =			
			25.4 h^{-1}			

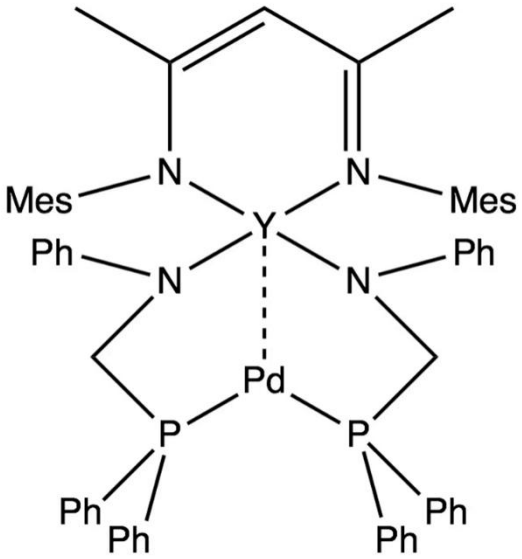

Supplementary Figure 3. The structure of Pd-Y single-source precursor (SSP) and the distance between Pd and Y is ~0.286 nm [11][24].

2.4. TEM results

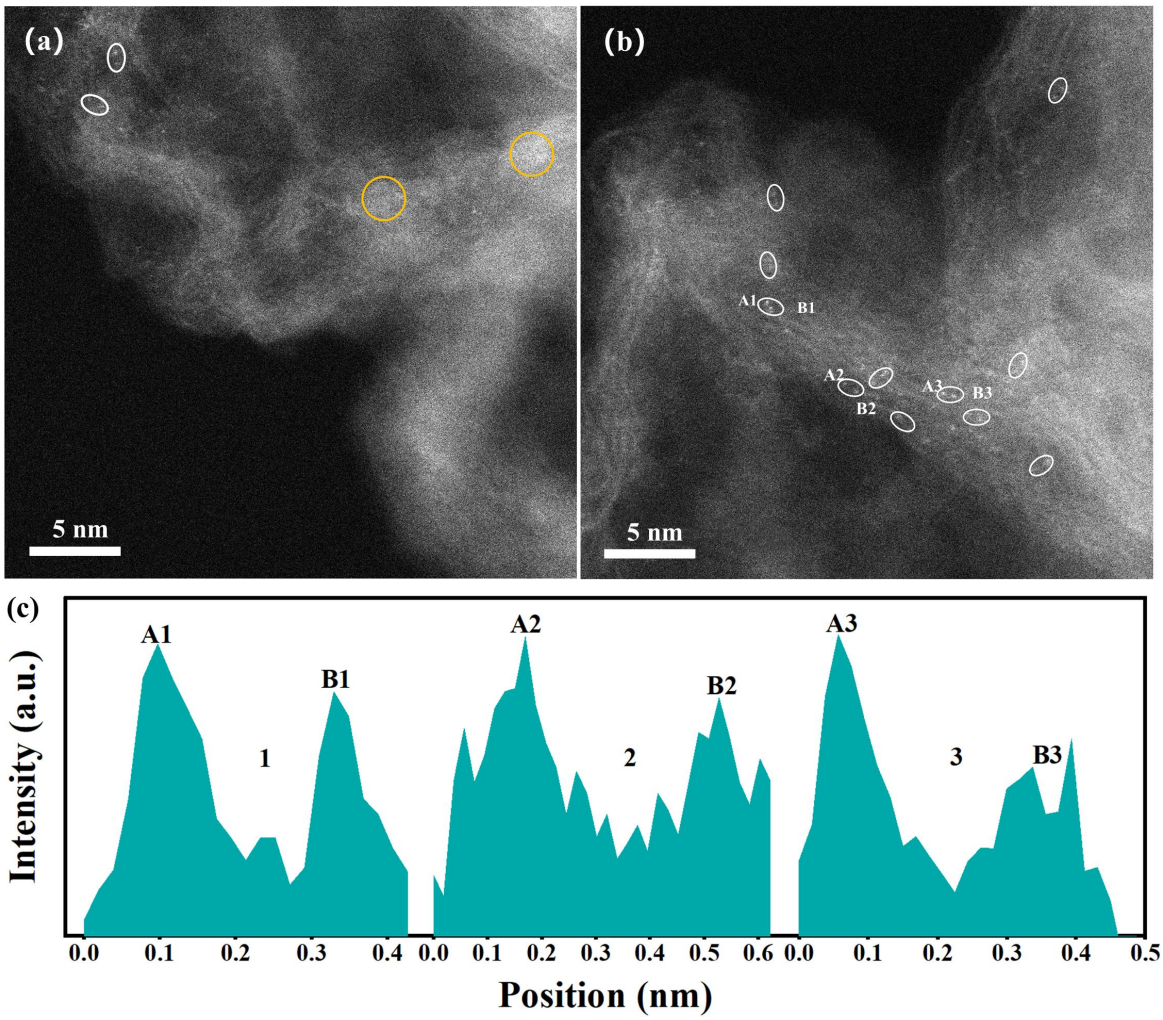

Supplementary Figure 4. The characterizations of 0.5%Pd-Y/C **(a)** Aberration-corrected HAADF-STEM images of 0.5%Pd-Y/C DAC (Pd-Y diatomic structures are emphasized by the white ovals, and Pd-Y clusters are marked with yellow circles); **(b)** images of Pd-Y diatomic pairs and **(c)** intensity distribution of ovals 1, 2, and 3 in image **(b)**.

2.5. Reaction order of H_2 and C_8H_6 over 0.02%Pd/C and exclusion of the mass/heat transfer limitations

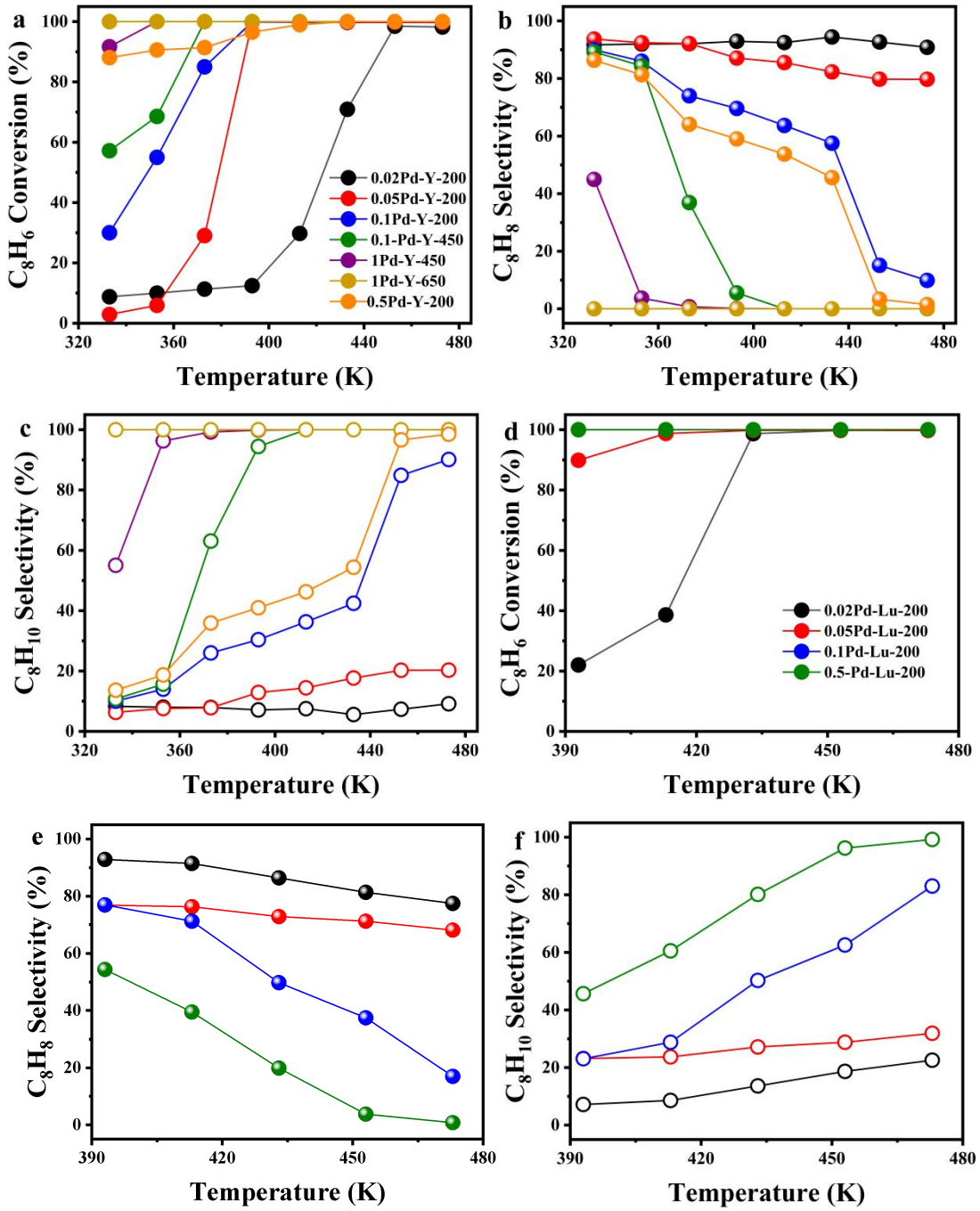

Supplementary Figure 5. Catalytic performance of xPd-Y/C-y (where x refers to the percentage value of Pd loading (x wt%), and y refers to the catalyst heat treatment temperature) in selective hydrogenation of phenylacetylene. **a** Phenylacetylene conversion, **b** styrene selectivity and **c** ethylbenzene selectivity as a function of reaction temperature. Catalytic performance of xPd-Lu/C-y (where x refers to the percentage value of Pd loading (x wt%), and y refers to the catalyst heat treatment

temperature) in selective hydrogenation of phenylacetylene. **d** Phenylacetylene conversion, **e** styrene selectivity and **f** ethylbenzene selectivity as a function of reaction temperature. Reaction condition: 30 kPa H_2, 0.3 kPa C_8H_6, 2.784 kPa C_6H_{12}, balance with Ar, 393 K-473 K, WHSV = 63.6 h^{-1}.

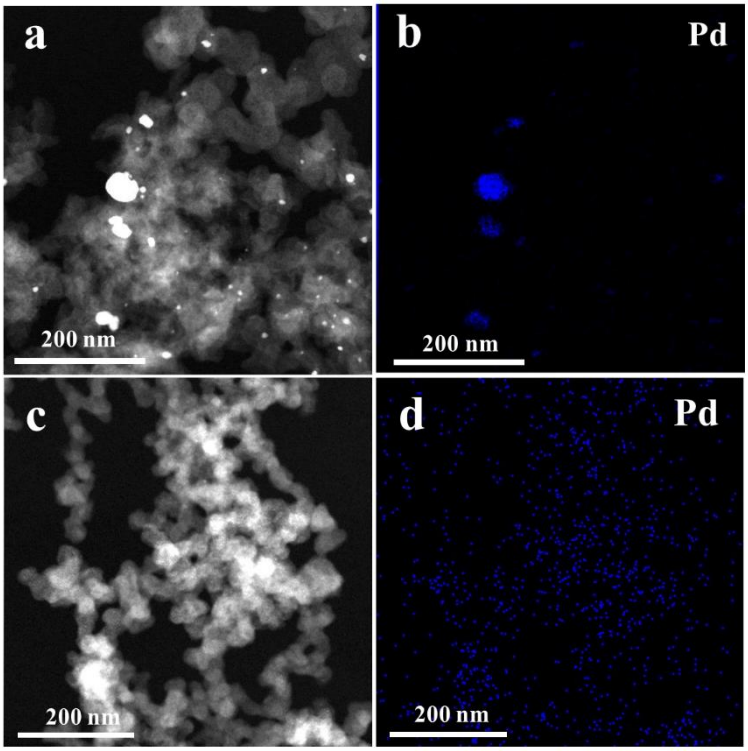

Supplementary Figure 6. Representative TEM image of **a** 1%Pd-Y/C-650 catalyst and the corresponding EDS mapping of **b** Pd element. Representative TEM image of **c** 1%Pd-Y/C-450 catalyst and the corresponding EDS mapping of **d** Pd element.

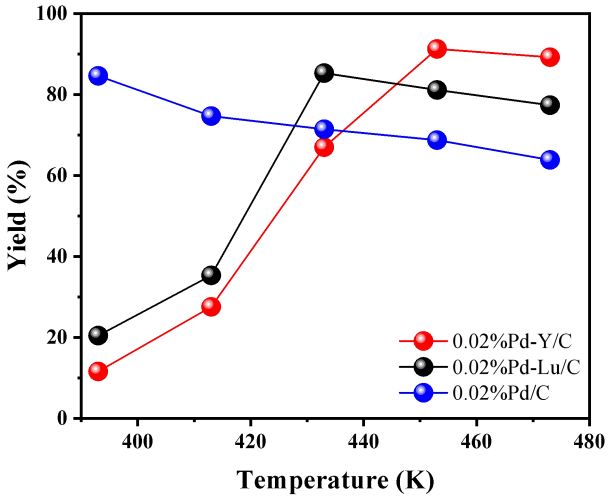

Supplementary Figure 7. The yield of styrene on different catalysts as a function of

temperature. Reaction condition: 30 kPa H_2, 0.3 kPa C_8H_6, 2.784 kPa C_6H_{12}, balance with Ar, 393-473 K, WHSV = 63.6 h^{-1}.

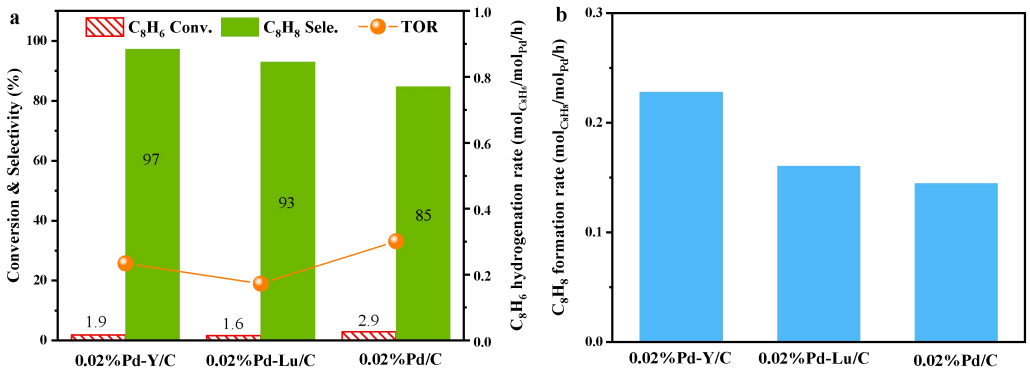

Supplementary Figure 8. Comparison of **a** phenylacetylene conversion, styrene selectivity, and phenylacetylene hydrogenation rate and **b** styrene formation rate over 0.02%Pd-Ln/C diatomic catalyst and 0.02%Pd/C single-atom catalyst. Reaction conditions: 30 kPa H_2, 0.3 kPa C_8H_6, 2.784 kPa C_6H_{12}, balance with Ar, 393 K, WHSV = 2162 h^{-1}, C_8H_6 conversion < 3%.

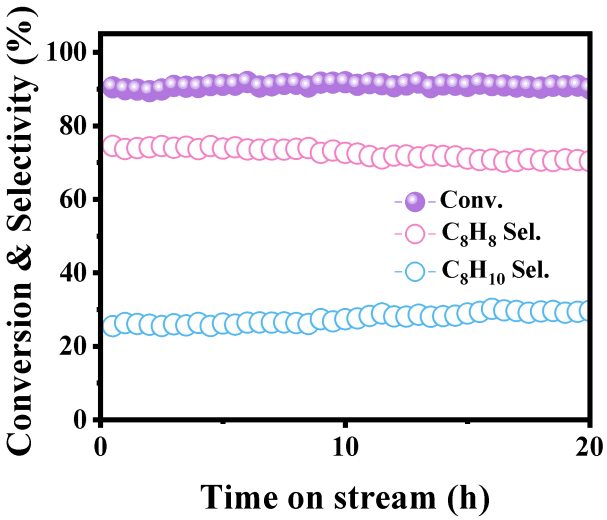

Supplementary Figure 9. Durability test on 0.02%Pd/C in the selective hydrogenation of phenylacetylene for 20 h at 393 K. Reaction conditions: 30 kPa H_2, 0.3 kPa C_8H_6, 2.784 kPa C_6H_{12}, balance with Ar, WHSV = 25.4 h^{-1}.

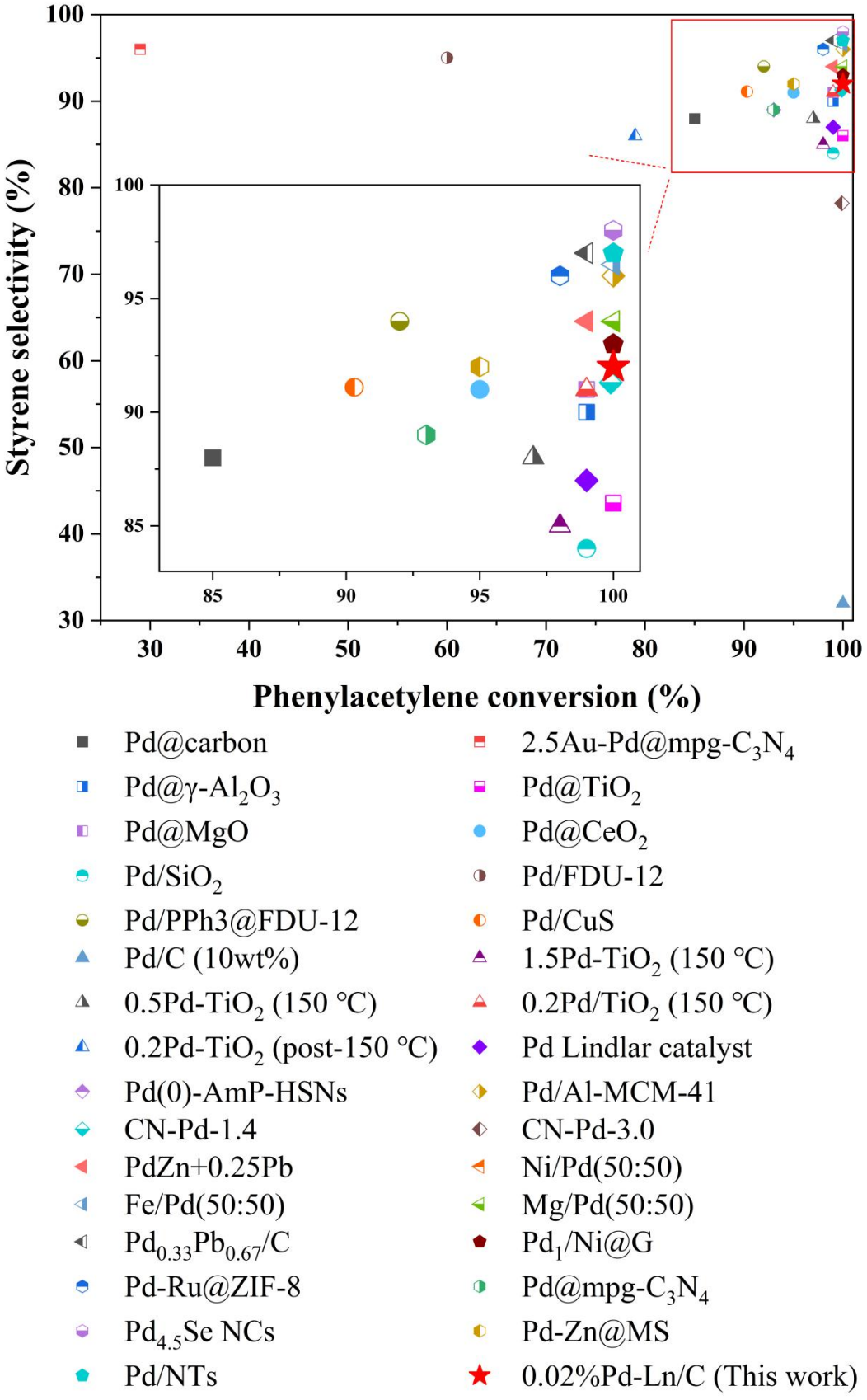

Supplementary Figure 10. Phenylacetylene conversion and styrene selectivity over various Pd-based catalysts.

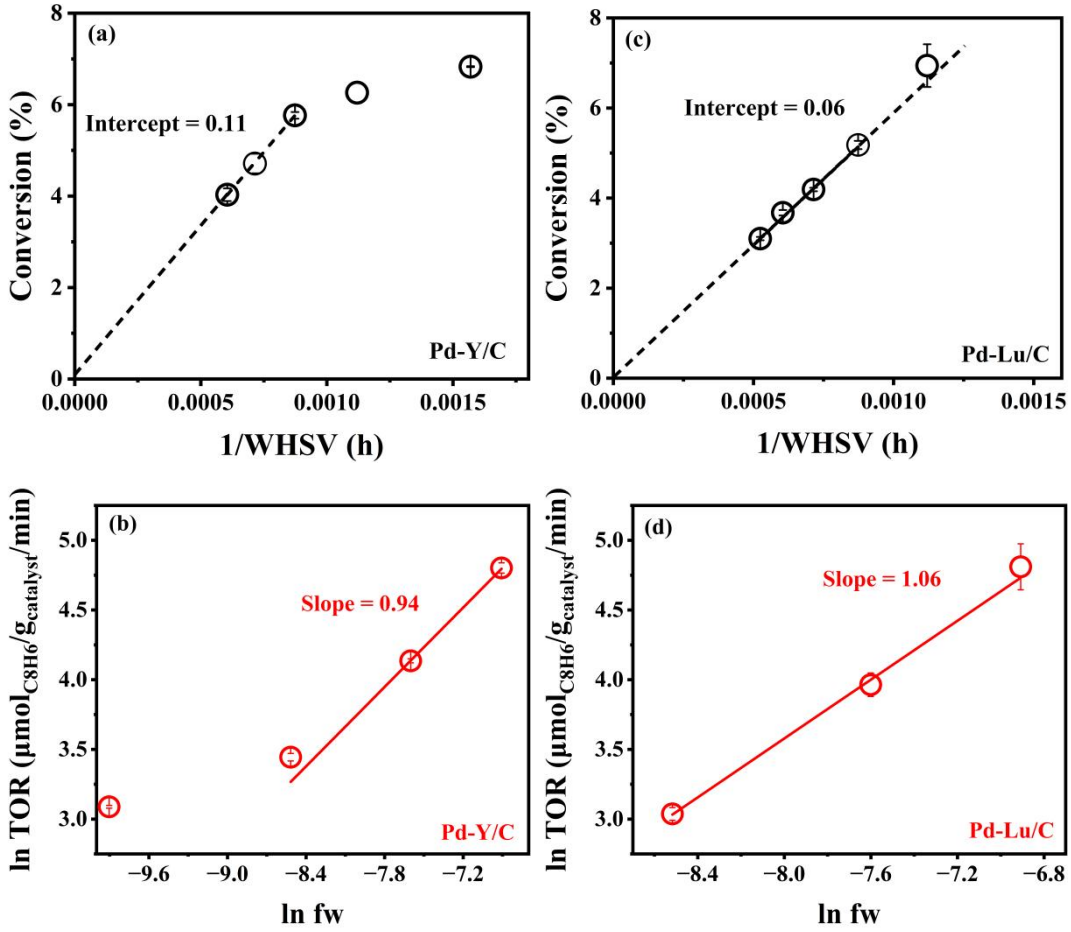

Supplementary Figure 11. a Increase reactants flow rate on 0.1%Pd-Y/C catalyst to eliminate diffusion resistance till intercept ~ 0 at 373 K. Reaction conditions: 30 kPa H_2, 0.3 kPa C_8H_6, 2.784 kPa C_6H_{12}, balance with Ar, 373 K, WHSV = 636-2162 h^{-1}. **b** Serial loading of x%Pd-Y/C (x=0.1, 0.05, 0.02) under a small contact time condition to exclude the transport limitations. Reaction conditions: 30 kPa H_2, 0.3 kPa C_2H_2, 2.784 kPa C_6H_{12}, balance with Ar, 373 K, WHSV = 2162 h^{-1}. **c** Increase reactants flow rate on 0.1%Pd-Lu/C catalyst to eliminate diffusion resistance till intercept ~ 0 at 373 K. Reaction conditions: 30 kPa H_2, 0.3 kPa C_2H_2, 2.784 kPa C_6H_{12}, balance with Ar, 373 K, WHSV = 636-2162 h^{-1}. **d** Serial loading of x%Pd-Lu/C (x=0.1, 0.05, 0.02 and 0.005) under a small contact time condition to exclude the transport limitations. Reaction conditions: 30 kPa H_2, 0.3 kPa C_8H_6, 2.784 kPa C_6H_{12}, balance with Ar, 373 K, WHSV = 2162 h^{-1}.

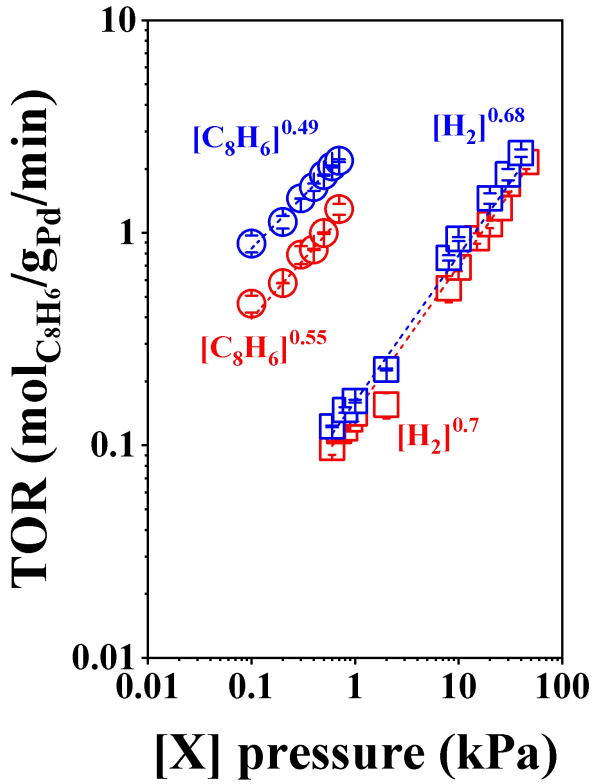

Supplementary Figure 12. Phenylacetylene hydrogenation reaction rates as a function of H_2 (363 K: red □; 373 K: blue □) (0.5~50 kPa H_2, 0.3 kPa C_8H_6, 2.784 kPa C_6H_{12}, balance with Ar, WHSV = 2162 h^{-1}) and C_8H_6 (363 K: red ○; 373 K: blue ○) (30 kPa H_2, 0.1~0.8 kPa C_8H_6, 2.784 kPa C_6H_{12}, balance with Ar, WHSV = 2162 h^{-1}) pressures over 0.02%Pd/C SA

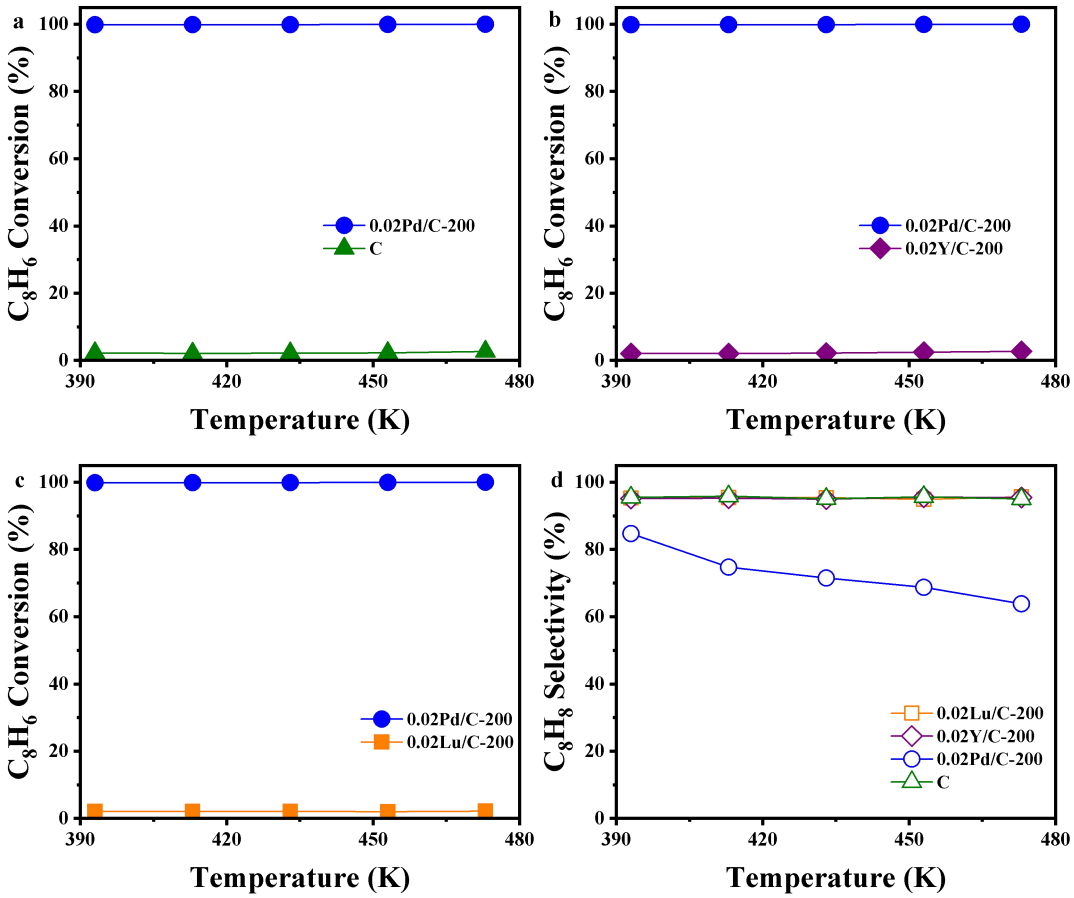

Supplementary Figure 13. Catalytic performance of 0.02%Pd/C, 0.02%Ln/C (Ln = Y/Lu) and carbon support in selective hydrogenation of phenylacetylene. Reaction condition: 30 kPa H_2, 0.3 kPa C_8H_6, 2.784 kPa C_6H_{12}, balance with Ar, 393 K-473 K, WHSV = 63.6 h^{-1}.

3. Discussion of kinetics and thermodynamics

Supplementary Note 1. Kinetic derivation

The scheme of the dissociative (Horiuti-Polanyi) hydrogenation mechanism is:

Step	Reaction	Constant
1	$C_8H_6 + * \rightleftharpoons C_8H_6*$	K_1
2	$H_2 + 2* \rightleftharpoons 2H*$	K_2
3	$C_8H_6* + H* \rightarrow C_8H_7* + *$	k_3
4	$C_8H_7* + H* \rightleftharpoons C_8H_8* + *$	K_4
5	$C_8H_8* \rightleftharpoons C_8H_8 + *$	K_5

Assuming H_2 dissociation (step 2) as the rete-limiting step, the rate of reaction can be written as:

$$\frac{r_{[H]}}{[L_{Pd}]} = \frac{k_2[H_2][*]^2}{[L_{Pd}]^2} \quad (S2)$$

Assuming that all the other elementary steps are in quasi-equilibrium, we have:

$$k_1[C_8H_6][*] = k_{-1}[C_8H_6*] \quad (S3)$$

$$k_3[C_8H_6*][H*] = k_{-3}[C_8H_7*][*] \quad (S4)$$

$$k_4[C_8H_7*][H*] = k_{-4}[C_8H_8*][*] \quad (S5)$$

$$k_5[C_8H_8*] = k_{-5}[C_8H_8][*] \quad (S6)$$

Leading to:

$$[C_8H_6*] = K_1[C_8H_6][*] \quad (S7)$$

$$[C_8H_7*] = \sqrt{\frac{K_1K_3[C_8H_6][C_8H_8]}{K_4K_5}}[*] \quad (S8)$$

$$[C_8H_8*] = \frac{[C_8H_8][*]}{K_5} \quad (S9)$$

$$[H*] = \sqrt{\frac{[C_8H_8]}{K_1K_3K_4K_5[C_8H_6]}}[*] \quad (S10)$$

The conservation of the total number of active sites leads to the site balance expressions:

$$[L_{Pd}] = [*] + [H*] + [C_8H_6*] + [C_8H_7*] + [C_8H_8*] \quad (S11)$$

Consequently, the resulting reaction rate is:

$$\frac{r_{[H]}}{[L_{Pd}]} = \frac{k_2[H_2][*]^2}{\left(1 + \sqrt{\frac{[C_8H_8]}{K_1K_3K_4K_5[C_8H_6]}} + K_1[C_8H_6] + \sqrt{\frac{K_1K_3[C_8H_6][C_8H_8]}{K_4K_5}} + \frac{[C_8H_8]}{K_5}\right)^2 [*]^2} \quad (S12)$$

At low conversions, the $[C_8H_8]$ is negligibly small, leading to a simplification of the rate expression:

$$\frac{r_{[H]}}{[L_{Pd}]} \approx \frac{k_2[H_2]}{(1 + K_1[C_8H_6])^2} \quad (S13)$$

The orders of reactions can be expressed as:

$$\mathrm{n}(H_2) = [H_2]\frac{\partial \ln \frac{r_{[H]}}{[L_{Pd}]}}{\partial [H_2]} = 1 \quad (S14)$$

$$\mathrm{n}(C_8H_6) = [C_8H_6]\frac{\partial \ln \frac{r_{[H]}}{[L_{Pd}]}}{\partial [C_8H_6]} = \frac{-2K_1[C_8H_6]}{1 + K_1[C_8H_6]} \quad (S15)$$

Thus, $n(H_2) = 1 \ \ and \ -2 \le n(C_8H_6) \le 0$.

Assuming the first hydrogen addition (step 3) of the Horiuti-Polanyi scheme as the rate-limiting step. The initial rate expression can be written as:

$$\frac{r}{[L_{Pd}]} = \frac{k_3[C_8H_6*][H*]}{[L_{Pd}]^2} \quad (S16)$$

Assuming that all the other elementary steps are in quasi-equilibrium, we have:

$$k_1[C_8H_6][*] = k_{-1}[C_8H_6*] \quad (S17)$$

$$k_2[H_2][*]^2 = k_{-2}[H*]^2 \quad (S18)$$

$$k_4[C_8H_7*][H*] = k_{-4}[C_8H_8*][*] \quad (S19)$$

$$k_5[C_8H_8*] = k_{-5}[C_8H_8][*] \quad (S20)$$

Leading to:

$$[C_8H_6{*}] = K_1[C_8H_6][*] \quad (S21)$$

$$[C_8H_7{*}] = \frac{[C_8H_8][*]}{K_4K_5\sqrt{K_2}[H_2]^{\frac{1}{2}}} \quad (S22)$$

$$[C_8H_8{*}] = \frac{[C_8H_8][*]}{K_5} \quad (S23)$$

$$[H{*}] = \sqrt{K_2}[H_2]^{\frac{1}{2}}[*] \quad (S24)$$

The conservation of the total number of active sites leads to the site balance expressions:

$$[L_{Pd}] = [*] + [H{*}] + [C_8H_6{*}] + [C_8H_7{*}] + [C_8H_8{*}] \quad (S25)$$

Consequently, the resulting reaction rate is:

$$\frac{r}{[L_{Pd}]} = \frac{k_3K_1\sqrt{K_2}[H_2]^{\frac{1}{2}}[C_8H_6][*]^2}{\left(1+\sqrt{K_2}[H_2]^{\frac{1}{2}} + K_1[C_8H_6] + \frac{[C_8H_6]}{K_4K_5\sqrt{K_2}[H_2]^{\frac{1}{2}}} + \frac{[C_8H_8]}{K_5}\right)^2[*]^2} \quad (S26)$$

At low conversions, the $[C_8H_8]$ is negligibly small, leading to a simplification of the rate expression:

$$\frac{r}{[L_{Pd}]} \approx \frac{k_3K_1\sqrt{K_2}[H_2]^{\frac{1}{2}}[C_8H_6]}{\left(1+\sqrt{K_2}[H_2]^{\frac{1}{2}} + K_1[C_8H_6]\right)^2} \quad (S27)$$

The orders of reactions can be expressed as:

$$n(H_2) = [H_2]\frac{\partial \ln \frac{r}{[L_{Pd}]}}{\partial [H_2]} = \frac{1+K_1[C_8H_6]-\sqrt{K_2}[H_2]^{\frac{1}{2}}}{2\left(1+K_1[C_8H_6]+\sqrt{K_2}[H_2]^{\frac{1}{2}}\right)} \quad (S28)$$

$$n(C_8H_6) = [C_8H_6]\frac{\partial \ln \frac{r}{[L_{Pd}]}}{\partial [C_8H_6]} = \frac{1-K_1[C_8H_6]+\sqrt{K_2}[H_2]^{\frac{1}{2}}}{1+K_1[C_8H_6]+\sqrt{K_2}[H_2]^{\frac{1}{2}}} \quad (S29)$$

Thus, $-0.5 \le n(H_2) \le 0.5$ *and* $-1 \le n(C_8H_6) \le 1$.

Assuming the second hydrogen addition (step 4) of the Horiuti-Polanyi scheme as the rate-limiting step. The initial rate expression can be written as:

$$\frac{\mathrm{r}}{[L_{Pd}]} = \frac{k_4[C_8H_7{*}][H{*}]}{[L_{Pd}]^2} \qquad (S30)$$

Assuming that all the other elementary steps are in quasi-equilibrium, we have:

$$\mathrm{k}_1[C_8H_6][{*}] = k_{-1}[C_8H_6{*}] \qquad (S31)$$

$$\mathrm{k}_2[H_2][{*}]^2 = k_{-2}[H{*}]^2 \qquad (S32)$$

$$k_3[C_8H_6{*}][H{*}] = k_{-3}[C_8H_7{*}][{*}] \qquad (S33)$$

$$k_5[C_8H_8{*}] = k_{-5}[C_8H_8][{*}] \qquad (S34)$$

Leading to:

$$[C_8H_6{*}] = K_1[C_8H_6][{*}] \qquad (S35)$$

$$[C_8H_7{*}] = K_1\sqrt{K_2}K_3[C_8H_6][H_2]^{\frac{1}{2}}[{*}] \qquad (S36)$$

$$[C_8H_8{*}] = \frac{[C_8H_8][{*}]}{K_5} \qquad (S37)$$

$$[H{*}] = \sqrt{K_2}[H_2]^{\frac{1}{2}}[{*}] \qquad (S38)$$

The conservation of the total number of active sites leads to the site balance expressions:

$$[L_{Pd}] = [{*}] + [H{*}] + [C_8H_6{*}] + [C_8H_7{*}] + [C_8H_8{*}] \qquad (S39)$$

Consequently, the resulting reaction rate is:

$$\frac{\mathrm{r}}{[L_{Pd}]} = \frac{k_4K_1K_2K_3[H_2][C_8H_6][{*}]^2}{\left(\begin{array}{l}1+\sqrt{K_2}[H_2]^{\frac{1}{2}} + K_1[C_8H_6] + \\ K_1\sqrt{K_2}K_3[C_8H_6][H_2]^{\frac{1}{2}} + \dfrac{[C_8H_8]}{K_5}\end{array}\right)^2} \qquad (S40)$$

At low conversions, the [C_8H_8] is negligibly small, leading to a simplification of the rate expression:

$$\frac{\mathrm{r}}{[L_{Pd}]} \approx \frac{k_4 K_1 K_2 K_3 [H_2][C_8H_6]}{\left(1+\sqrt{K_2}[H_2]^{\frac{1}{2}} + K_1[C_8H_6] + K_1\sqrt{K_2}K_3[C_8H_6][H_2]^{\frac{1}{2}}\right)^2} \quad (S41)$$

The orders of reactions can be expressed as:

$$n(H_2) = [H_2]\frac{\partial \ln \frac{r}{[L_{Pd}]}}{\partial [H_2]} = \frac{1+K_1[C_8H_6]-\sqrt{K_2}[H_2]^{\frac{1}{2}}}{1+K_1[C_8H_6]+\sqrt{K_2}[H_2]^{\frac{1}{2}}} \quad (S42)$$

$$n(C_8H_6) = [C_8H_6]\frac{\partial \ln \frac{r}{[L_{Pd}]}}{\partial [C_8H_6]} = \frac{1-K_1[C_8H_6]+\sqrt{K_2}[H_2]^{\frac{1}{2}}}{1+K_1[C_8H_6]+\sqrt{K_2}[H_2]^{\frac{1}{2}}} \quad (S43)$$

Thus, $0 \le \mathrm{n}(H_2) \le 1$ *and* $-1 \le n(C_8H_6) \le 1$.

Supplementary Note 2 Derivation of rate-determining steps for the hydrogenation of phenylacetylene over 0.02%Pd/C SAC

For 0.02%Pd/C SAC, "C_8H_7* + H*" elementary step (step 4) is hypothesized to be the kinetically relevant step, by regarding the QE assumption on C_8H_6 adsorption, H_2 dissociation and C_8H_8 desorption, the active species would be denoted as below:

$$[L_{Pd}] = [*] + [H*] + [C_8H_6*] + [C_8H_7*] + [C_8H_8*]$$

(S44)

and the formation rate of C_8H_8 will be denoted as:

$$\frac{\mathrm{r}}{[L_{Pd}]} = \frac{k_4 K_1 K_2 K_3 [H_2][C_8H_6][*]^2}{\left(1+\sqrt{K_2}[H_2]^{\frac{1}{2}} + K_1[C_8H_6] + K_1\sqrt{K_2}K_3[C_8H_6][H_2]^{\frac{1}{2}} + \frac{[C_8H_8]}{K_5}\right)^2 [*]^2}$$

(S45)

with the QE assumption and the full derivation of the rate expression as shown in **Supplementary Note 1**, equation (S45) could be denoted as:

$$\frac{\mathrm{r}}{[L_{Pd}]} \approx \frac{k_4 K_1 K_2 K_3 [H_2][C_8H_6]}{\left(1+\sqrt{K_2}[H_2]^{\frac{1}{2}} + K_1[C_8H_6] + K_1\sqrt{K_2}K_3[C_8H_6][H_2]^{\frac{1}{2}}\right)^2} \quad (S46)$$

In equation (S46), the term in the numerator of the rate equation depicts the steps that each product takes, while the denominator denotes the site balance over sites occupied by H_2, C_8H_6 and C_8H_6-derived intermediates and empty sites (*). When [C_8H_6] is low, the number of empty sites (which are most likely occupied by H_2 and C_8H_6) is larger than that of C_8H_6 intermediates, then equation (S46) predicts first-order dependence on C_8H_6. When [C_8H_6] is high, the C_8H_6-derived intermediates become MARIs and equation (S46) assumes the form where the rates are either zero or negative first-order on C_8H_6 pressure; furthermore, at low conversion, [C_8H_8] is negligible, by supposing that different species are the MASIs, the rate expression simplifies to either zero or first-order in H_2. The kinetic derivations are in good consistent with acquired experimental results. Therefore, it indicated that "C_8H_7* + H*" (step 4) is the RDS for 0.02%Pd/C catalyst.

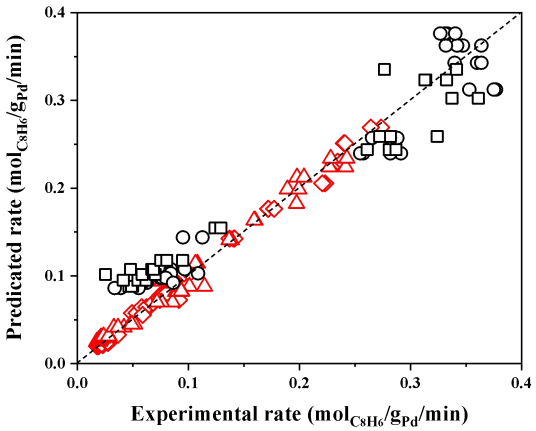

Supplementary Figure 14. Parity plot between predicated and experimental rate of phenylacetylene hydrogenation over 0.02%Pd-Y/C (marked in black) and 0.02%Pd-Lu/C (marked in red) catalysts at 363 K and 373 K by varying the partial pressure of C_8H_6 and H_2.

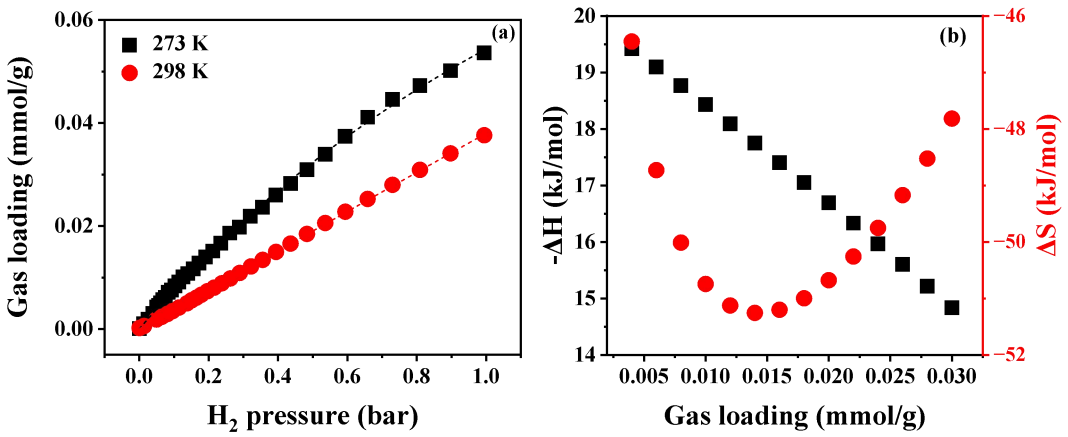

Supplementary Figure 15. a Adsorption isotherms of H_2 on 0.02%Pd-Y/C. **b** Heats of adsorption and ΔS as a function of H_2 adsorption amount.

Supplementary Table 4. The corrected rate and equilibrium constants of C_8H_6 hydrogenation on 0.02%Pd-Y/C catalyst

Catalyst	T/K	Rate and equilibrium constants[a]		
		K_3/s^{-1}	K_1/kPa^{-1}	K_2/kPa^{-1}
0.02%Pd-Y/C	373	6.5	0.4	0.002
	363	5.0	0.6	0.004

[a] The equilibrium constant K_2 is obtained by the ideal gas isothermal equation based on the measured heat of H_2 adsorption, and other parameters are obtained by parity fitting after K_2 correction.

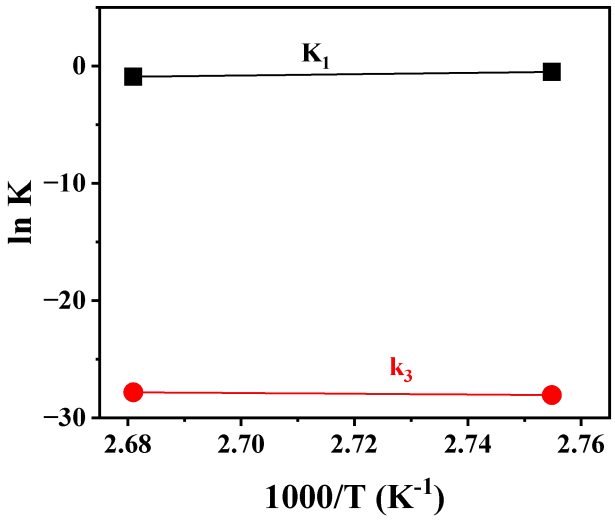

Supplementary Figure 16. Temperature dependences for rate and equilibrium constants for C_8H_6 hydrogenation over 0.02%Pd-Y/C catalyst at 363-373 K.

Supplementary Table 5. Energetic parameters for C_8H_6 hydrogenation on 0.02%Pd-Y/C at 363-373 K

Catalyst	Enthalpy (kJ/mol) [a]		
	ΔH_1	ΔH_2	$\Delta H_3^{\neq}$
0.02%Pd-Y/C	-45.6	-17.2	69.5

[a] ΔH_2 is obtained by calculating the adsorption heat of H_2, $\Delta H_3^{\neq}$ is calculated by activation energy of 0.02%Pd-Y/C and other energy parameters were obtained by calculating the kinetic parameters obtained by corresponding parity fitting.

Supplementary Note 3. Regression kinetic and thermodynamic constants derive related energies.

The kinetic parameters consisting of rate constants and equilibrium constants can be achieved by parity fitting. Prior to regression, we first use thermodynamic methods to determine K_2, that is, the equilibrium constant of dissociated H_2 adsorption on 0.02%Pd-Y/C diatomic catalyst (**Supplementary Figure 15**). The rate and equilibrium constants obtained by parity fitting are corrected by K_2 calculated by H_2 isothermal adsorption determined by experiments, which leads to more accurate fitting results. As displayed in **Supplementary Figure 16**, we calculate the enthalpy and entropy of H_2 adsorption by using equation (S47):

$$\ln P = \frac{\Delta H}{RT} - \frac{\Delta S}{R} \quad (S47)$$

where P is the pressure of hydrogen, T is the absolute temperature, R is the ideal gas constant. The enthalpy difference (ΔH) and the entropy of adsorption (ΔS) are determined by the slope and intercept of the fitted line with 1/T at constant gas loading, respectively. For 0.02%Pd-Y/C, the value of ΔH_2 = -17.2 kJ/mol, that is, the heat released by H_2 during adsorption is 17.2 kJ/mol. K_2 is then calculated according to equation (S48) and equation (S49) at 363 K and 373 K, and the values of K_2 are 0.004 and 0.002, respectively.

$$\Delta G = \Delta H - T\Delta S \quad (S48)$$

$$K_2 = \exp\left(-\frac{\Delta G}{RT}\right) \quad (S49)$$

The rate constant (k_3) and equilibrium constants (K_1 and K_2) obtained by after correction by K_2 are displayed in **Table S4**. The temperature dependence of equilibrium constants and rate constant are displayed in **Supplementary Figure 16**. The energetic parameters (ΔH_1, ΔH_2 and ΔH_3) derived from equation (S50) and equation (S51) are listed in **Supplementary Table 5**.

$$k = \frac{k_B T}{h} \cdot K^{\neq} \quad (S50)$$

where k is the rate constant, k_B is the Boltzman's constant, h is the Planck's constant, $K^{\neq}$ is the equilibrium constant.

$$\ln K^{\neq} = -\frac{\Delta H}{R} \cdot \frac{1}{T} + \frac{\Delta S^{\neq}}{R} \quad (S51)$$

Supplementary Table 6. Comparison of apparent activation energies of Pd catalysts in reference

Apparent activation energy of Pd catalysts (kJ/mol)	Reference
33.5	[13][25]
38.9	[14][26]
39.3	[14][26]
46	[14][26]
64.3	[2]

4. Reference

1. Ravel B, Newville M. ATHENA, ARTEMIS, HEPHAESTUS: data analysis for X-ray absorption spectroscopy using IFEFFIT. *J Synchrotron Radiat* 2005;12:537-41. https://dx.doi.org/10.1107/S0909049505012719
2. Zhao LM, Qin XT, Zhang XR,et al. A magnetically separable Pd single-atom catalyst for efficient selective hydrogenation of phenylacetylene. *Adv Mater* 2022;34:2110455-62. https://dx.doi.org/10.1002/adma.202110455
3. Yang F, Ding SP, Song HB, et al. Single-atom Pd dispersed on nanoscale anatase TiO_2 for the selective hydrogenation of phenylacetylene. *Sci China Mater* 2020;63:982-92. https://dx.doi.org/10.1007/s40843-020-1271-x
4. Li ZX, Hu ML, Liu JH, et al. Mesoporous silica stabilized MOF nanoreactor for highly selective semi-hydrogenation of phenylacetylene via synergistic effect of Pd and Ru single site. *Nano Res* 2022;15:1983-92. https://dx.doi.org/10.1007/s12274-021-3849-2
5. Deng DS, Yang Y, Gong YT, et al. Palladium nanoparticles supported on mpg-C_3N_4 as active for semihydrogenation of phenylacetylene under mild conditions. *Green Chem* 2013;15:2525-31. https://dx.doi.org/10.1039/c3gc40779a
6. Wang ML, Liang LL, Liu X, et al. Selective semi-hydrogenation of alkynes on palladium-selenium nanocrystals. *J Catal* 2023;418:247-55. https://dx.doi.org/10.1016/j.jcat.2023.01.024
7. Li ZX, Hu ML, Liu BW, et al. Pd-Zn Alloy Nanoparticles Encapsulated into Mesoporous Silica with Confinement Effect for Highly Selective Semi-

Hydrogenation of Phenylacetylene. *ChemCatChem* 2021;13:868-73. https://dx.doi.org/10.1002/cctc.202001159

8. Liu Y, Guo W, Li XJ, et al. Copper Single-Atom-Covered Pt Nanoparticles for Selective Hydrogenation of Phenylacetylene. *ACS Appl Nano Mater* 2021;4:5292-300. https://dx.doi.org/10.1021/acsanm.1c00646
9. Jin Y, Wang PT, Mao XN, et al. A Top-Down Strategy to Realize Surface Reconstruction of Small-Sized Pt-Based Nanoparticles for Selective Hydrogenation. *Angew Chem Int Ed* 2021;60:17430-4. https://dx.doi.org/10.1002/anie.202106459
10. Shao LD, Huang X, Teschner D, et al. Gold Supported on Graphene Oxide: An Active and Selective Catalyst for Phenylacetylene Hydrogenations at Low Temperatures. *ACS Catal* 2014;4:2369-73. https://dx.doi.org/10.1021/cs5002724
11. Jackson SD, Shaw LA, et al. The liquid-phase hydrogenation of phenylacetylene and styrene on a palladium/carbon catalyst. *Appl Catal A* 1996;134:91-9. https://dx.doi.org/10.1016/0926-860X(95)00194-8
12. Weerachawanasak P, Mekasuwandumrong O, Arai M, et al. Effect of strong metal-support interaction on the catalytic performance of Pd/TiO_2 in the liquid-phase semihydrogenation of phenylacetylene. *J Catal* 2009;262:199-205. https://dx.doi.org/10.1016/j.jcat.2008.12.011
13. Kuwahara Y, Kango H, Yamashita H. Pd nanoparticles and aminopolymers confined in hollow silica spheres as efficient and reusable heterogeneous catalysts

for semihydrogenation of alkynes. *ACS Catal* 2019;9:1993-2006. https://dx.doi.org/10.1021/acscatal.8b04653

14. Guo M, Li H, Ren YQ, et al. Improving catalytic hydrogenation performance of Pd nanoparticles by electronic modulation using phosphine ligands. *ACS Catal* 2018;8:6476-85. https://dx.doi.org/10.1021/acscatal.8b00872
15. Wang Y, Chen Z, Shen RA, et al. Pd-dispersed CuS hetero-nanoplates for selective hydrogenation of phenylacetylene. *Nano Res* 2016;9:1209-19. https://dx.doi.org/10.1007/s12274-016-1016-y
16. Verho O, Zheng H, Gustafson KPJ, et al. Application of Pd nanoparticles supported on mesoporous hollow silica nanospheres for the efficient and selective semihydrogenation of alkynes. *ChemCatChem* 2016;8:773-8. https://dx.doi.org/10.1002/cctc.201501112
17. Tiengchad N, Mekasuwandumrong O, Na-Chiangmai C, et al. Geometrical confinement effect in the liquid-phase semihydrogenation of phenylacetylene over mesostructured silica supported Pd catalysts. *Catal Commun* 2011;12:910-6. https://dx.doi.org/10.1016/j.catcom.2011.01.029
18. Ma L, Jiang P, Wang K, et al. Phosphorus and nitrogen-doped palladium nanomaterials support on coral-like carbon materials as the catalyst for semi-hydrogenation of phenylacetylene and mechanism study. *J Alloys Compd* 2021;868:159047-56. https://dx.doi.org/10.1016/j.jallcom.2021.159047
19. Miyazaki M, Furukawa S, Takayama T, et al. Surface modification of PdZn nanoparticles via galvanic replacement for the selective hydrogenation of terminal

alkynes. *ACS Appl Nano Mater* 2019;2:3307-14. https://dx.doi.org/10.1021/acsanm.9b00761

20. Dominguezdominguez S, Berenguermurcia A, Cazorlaamoros D. Semihydrogenation of phenylacetylene catalyzed by metallic nanoparticles containing noble metals. *J Catal* 2006;243:74-81. https://dx.doi.org/10.1016/j.jcat.2006.06.027
21. Liu J, Zhu YN, Liu C, et al. Excellent selectivity with high conversion in semi-hydrogenation of alkynes using Pd-based bimetallic catalysts. *ChemCatChem* 2017;9:4053-57. https://dx.doi.org/10.1002/cctc.201700800
22. Zhao LM, Qin XT, Zhang XR, et al. A magnetically separable Pd single-atom catalyst for efficient selective hydrogenation of phenylacetylene. *Adv Mater* 2022;34:2110455-62. https://dx.doi.org/10.1002/adma.202110455
23. Dominguez S, Bhabendra AnBM, Pradhan K, et al. Semihydrogenation of phenylacetylene catalyzed by palladium nanoparticles supported on carbon materials. *J Phys Chem C* 2008;112:3827-34. https://dx.doi.org/10.1021/jp710693u
24. Cui P, Wu C, Du J, et al. Three-coordinate Pd(0) with rare-earth metalloligands: Synergetic CO activation and double P-C bond cleavage-formation reactions. *Inorg Chem* 2021;60:9688-99. https://dx.doi.org/10.1021/acs.inorgchem.1c00990
25. Shutt E, Winterbottom JM. Heterogeneous catalysis in the liquid phase. *Platinum Met Rev* 1971;15:94-9. https://dx.doi.org/10.1595/003214071X1539499

26. Aramendia MA, Borau V, Jimenex C, et al. Optimization of the selective semi-hydrogenation of phenylacetylene with supported palladium systems. *Appl Catal* 1990;63:375-89. https://dx.doi.org/10.1016/S0166-9834(00)81726-1